Libyan Journal of Applied and Contemporary Sciences
ISSN
E: 3136-3709
L: 3136-3695
Vol 1: No 2

Analytical Assessment of Corona Discharge and Skin-Effect Contributions to the Efficiency of 220 kV Overhead Transmission Lines

Adel M Almedhem

Department of Electrical and Electronic Engineering, The Higher Institute of Engineering Technology-Zliten, Libya

Email corresponding author's: adel.almedhim@hpiz.edu.ly

Received: 24/9/2026 Accepted: 4/11/2026 Published: 6/11/2026

Abstract

Corona discharge can be a first-order loss mechanism on high-voltage overhead lines, whereas the skin-effect contribution at 50 Hz is expected to be secondary for the conductor sizes considered here. This paper quantifies both effects for a 220 kV, 50 Hz, 100 km line using an analytical screening model. Three phase configurations are compared: a single ACSR Panther conductor, a single ACSR Zebra conductor and a twin-bundle Zebra. Surface gradients are calculated for an equivalent horizontal geometry and compared with corona-onset gradients for fair weather and heavy rain, at sea level and at 2000 m. Corona loss is estimated with Peek's formula, and alternating-current resistance follows the IEC 60287 skin- and proximity-effect expressions, checked against a solid-conductor Bessel-function solution. At a delivered load of 150 MW and a power factor of 0.95, skin effect raises conductor resistance by 0.30% for Panther and 1.20% for Zebra, yet lowers efficiency by only 0.015–0.032 percentage points. Corona is negligible in fair weather at sea level for both Zebra designs. In heavy rain, however, it reaches 28.1 kW/km for Panther and 2.95 kW/km for single Zebra, and it grows sharply at altitude and under voltage excursions to 245 kV. The twin-bundle Zebra stays corona-free at nominal voltage in every sea-level scenario and achieves the highest efficiency, 98.59%. The model deliberately omits phase-specific field asymmetry, shield wires, local hardware enhancement, surface contamination and time-varying weather, loading and temperature; its numerical predictions should therefore be interpreted as screening values. Within that scope, conductor choice, bundling and altitude derating govern the corona penalty, while skin effect is retained mainly to establish its small practical contribution.

Keyword : *220 kV transmission line; corona loss; skin effect; transmission efficiency; ACSR conductors; bundled conductors; Peek's formula*

Doi : https://doi.org/10.64943/ljacs.2026.010221

Copyright © 2026 Author(s) ; Published by Libyan Journal of Applied and Contemporary Sciences
This is an open access article licensed under CC BY: (https://creativecommons.org/licenses/by/4.0)

INTRODUCTION

Overhead high-voltage alternating-current (HVAC) lines remain the backbone of bulk power delivery. The 220 kV class is widely used for regional transmission, for linking large load centres and for evacuating mid-sized generation. Energy lost on these lines is energy that is generated but never sold, so even small gains in efficiency bring lasting savings and reduce the generation required [1,2]. Most of the loss is Joule heating in the conductors, but additional mechanisms depend on voltage, conductor geometry, frequency, atmospheric condition and surface state. Corona discharge can become a dominant incremental loss when the surface field exceeds the local onset threshold, while skin effect modifies the resistive loss through the frequency-dependent current distribution [3-6].

Corona is a partial breakdown of the air around a conductor. It begins when the electric field at the conductor surface exceeds the local ionisation threshold. Besides dissipating real power, it produces audible noise, radio and television interference, and ozone and other oxidants, and it can speed up the ageing of line hardware [3-5]. Weather matters a great deal: raindrops, fog and surface contamination create field-enhancing points that can raise losses substantially above fair-weather values [4,5]. Dust accumulation, industrial pollution, conductor surface degradation and ageing can produce a similar

field-intensification effect, while suspension fittings, clamps, corona rings and bundle spacers create local geometric discontinuities that are not represented by a smooth-conductor field calculation [4,5]. Skin effect is a different electromagnetic phenomenon. It pushes alternating current towards the conductor surface, shrinking the effective cross-section and raising the effective resistance [6, 9]. It depends on conductor size, material and frequency. At 50/60 Hz it is usually small, but it becomes more noticeable for large-diameter conductors; its practical importance must nevertheless be judged against the much larger baseline Joule loss.

At 220 kV both effects are physically present, but they need not have comparable engineering significance. The operating field can be high enough for a single small-diameter conductor to reach or exceed the corona-onset gradient in bad weather or at altitude. By contrast, the calculated skin-effect increase is expected to be small relative to the baseline Joule loss at 50 Hz. The practical question is therefore twofold: how much of the loss budget do corona and skin effect consume under the stated scenarios, and which design measures—conductor size, bundling and altitude derating—control the materially important part of that loss?

This paper addresses that question with a transparent analytical screening model built on standard formulas. It makes four contributions. First, it formulates the surface gradient, corona onset and loss, and ac resistance in a single framework that applies to single and bundled conductors. Second, it compares three representative 220 kV configurations under fair weather, heavy rain, 2000 m altitude and a 245 kV voltage excursion. Third, it decomposes efficiency into baseline Joule loss, skin-effect loss and weather-weighted corona loss, and tests sensitivity to the assumed foul-weather fraction. Fourth, it identifies explicitly which effects are outside the model—phase-to-phase field asymmetry, overhead shield wires, local enhancement at fittings and spacers, ACSR strand/core electromagnetic detail, surface contamination and ageing, and time-varying weather, loading and temperature—so that the numerical results are not interpreted as a substitute for project-specific electromagnetic, thermal or statistical design studies.

The paper is organised as follows. Section 2 gives the theoretical background, and Section 3 describes the system data, equivalent geometry and modelling assumptions. Section 4 presents and discusses the results, including the practical magnitude of the skin-effect contribution relative to baseline Joule loss. Section 5 summarises mitigation measures, Section 6 records the analytical limitations and required validation steps, and Section 7 concludes.

THEORETICAL BACKGROUND

Corona discharge and corona power loss

The ionisation threshold of air depends on the relative air density factor δ, which accounts for the pressure b (cm Hg) and the temperature t (°C):

$$\delta = \frac{3.92\, b}{273 + t} \tag{1}$$

Following Peek [3], the disruptive (onset) gradient at the conductor surface is expressed as a peak value in kV/cm:

$$E_0 = 30\, m\, \delta \tag{2}$$

where m is the surface irregularity factor. New stranded conductors in fair weather typically have m of about 0.8–0.87, while values of 0.6 or lower are commonly adopted for heavy rain or heavily contaminated surfaces [3,5]. The visual onset gradient is higher by the factor $(1 + 0.301/\sqrt{(\delta\, r)})$, with r in cm. The disruptive value of Eq. (2) is used here because it marks the onset of measurable power loss.

The peak surface gradient of a phase with n subconductors of radius r on a bundle circle of radius R follows from the phase charge per unit length. In Eq. (3), V_{ph} is the rms phase-to-neutral voltage, D the geometric mean distance between phases, r_{eq} the equivalent bundle radius and ε_0 the permittivity of free space:

$$E_{max} = \frac{Q}{2\pi\varepsilon_0 n r}\left[1 + \frac{(n-1)r}{R}\right],\quad Q = C\sqrt{2}\,V_{ph},\quad C = \frac{2\pi\varepsilon_0}{ln\left(\frac{D}{r_{eq}}\right)} \tag{3}$$

The critical (onset) phase voltage is then the phase voltage scaled by the ratio of the onset gradient to the actual surface gradient:

$$V_0 = V_{ph}\,\frac{E_0}{E_{max}} \tag{4}$$

When V_{ph} exceeds V_0, Peek's empirical expression gives the corona power loss per phase and per subconductor:

$$P_c = \frac{241}{\delta}(f + 25)\sqrt{\frac{r}{D}}(V - V_0)^2 \times 10^{-5} \tag{5}$$

where P_c is in kW/km, f is the supply frequency in Hz and voltages are in kV rms. For a bundle, the loss of one subconductor is multiplied by n, and for a three-phase line by three. Peek's expression was derived from laboratory and field tests at moderate ratios of V/V_0. It is widely used for screening studies, but it is less accurate at large ratios and for bundled geometries [4,5]. The results below are therefore best read as comparative estimates, not as predictions of measured loss.

Skin effect and alternating-current resistance

For a sinusoidal current of frequency f in a homogeneous conductor of resistivity ρ and permeability μ0, the classical skin depth is:

$$\delta_s = \sqrt{\frac{\rho}{\pi f \mu_0}} \tag{6}$$

For aluminium at 50 Hz, the skin depth is about 12.0 mm at 20 °C and 13.2 mm at 75 °C. The radius of a large ACSR conductor is of the same order, so a non-uniform current density can be expected in the aluminium portion. The exact solution for a homogeneous solid round conductor involves Bessel functions [9-11]. For engineering calculations, the IEC 60287 approximation [6] expresses the ac resistance as. In the present paper this expression is used as an effective-conductor screening approximation; it is not a strand-resolved electromagnetic model of ACSR and should not be read as one.

$$R_{ac} = R_{dc}\,(1 + y_s + y_p) \tag{7}$$

$$y_s = \frac{x^4}{192 + 0.8\,x^4},\quad x^2 = \frac{8\pi f \times 10^{-7}\,k_s}{R'} \tag{8}$$

where R′ is the dc resistance in Ω/m, ks = 1 for round stranded conductors, ys is the skin-effect factor and yp is the proximity-effect factor, which matters only for closely spaced subconductors. The auxiliary variable x is defined by the second expression in Eq. (8). Temperature enters through Rdc(T) = R20[1 + α(T − 20)], with α = 0.00403 K−1 for aluminium. For ACSR, this treatment replaces the concentric aluminium strands and galvanised-steel core by effective parameters. It therefore omits the

magnetic permeability of the steel core, the radial redistribution of current among aluminium layers and the helical lay of the strands; these features can be important when a conductor-specific ac-resistance model is required [7,12]. The present results consequently quantify the order of magnitude of the skin-effect contribution rather than providing a full ACSR electromagnetic solution.

Definition of transmission efficiency

Efficiency is the ratio of the delivered active power P_r to the sending-end power, which equals P_r plus the line losses:

$$\eta = \frac{P_r}{P_r + P_{Cu} + P_{cor}} \times 100\ \% \qquad (9)$$

where PCu = 3I2Racℓ is the conductor loss, Pcor is the weather-weighted corona loss, ℓ is the line length and Rac is the ac resistance per phase per kilometre. The skin-effect contribution is isolated by comparing η computed with Rac against η computed with Rdc. Because the same phase-gradient approximation is used for the three phases, Eq. (9) should be interpreted as a configuration-level screening efficiency; it does not include phase-specific corona margins, shield-wire coupling or local hardware losses.

SYSTEM MODEL AND METHODOLOGY

Line configurations and operating conditions

The study considers a 100 km, 50 Hz, 220 kV line with a horizontal flat phase arrangement and 6.5 m phase spacing, which gives a geometric mean distance of D = 8.19 m. Table 1 summarises the three phase-conductor configurations: a single ACSR Panther conductor, a single ACSR Zebra conductor and a twin bundle of ACSR Zebra with 0.40 m subconductor spacing. For the resistance calculation the conductor temperature is fixed at 75 °C, a common design operating temperature for ACSR [8]. The delivered power is varied between 50 and 250 MW at a power factor of 0.95 lagging, and the highest system voltage of 245 kV represents voltage excursions. The field calculation uses an equivalent conductor-to-ground geometry and applies the same Emax to all three phases. This is a deliberate screening simplification: in a horizontal arrangement, the centre phase can experience a different capacitance and field concentration from the outer phases, and the overhead shield wires and ground plane can modify the field distribution through electrostatic coupling [4,5,11]. The reported Emax is therefore a representative configuration value, not a phase-resolved worst-case value. Shield-wire coupling and ground-plane image effects are omitted and must be restored in a project-specific geometry model.

Table 1. Conductor data and calculated line parameters (75 °C, 50 Hz).

Configuration	d (mm)	R_{20} (Ω/km)	$R_{dc,75}$ (Ω/km)	y_s (%)	C (nF/km)	E_{max} at 220 kV (kV/cm)
Single ACSR Panther	21.00	0.1363	0.1665	0.30	8.35	25.69
Single ACSR Zebra	28.62	0.0674	0.0823	1.20	8.76	19.77
Twin ACSR Zebra (0.40 m)	28.62	0.0674	0.0823	1.20	11.88	14.36

d: conductor outer diameter; R_{20}: dc resistance at 20 °C per subconductor; $R_{dc,75}$: dc resistance at 75 °C per subconductor; y_s: skin-effect increase in ac resistance; C: phase capacitance to neutral; E_{max}: peak surface gradient. The Panther and Zebra data are typical catalogue values; manufacturer data should be substituted for a specific project.

Weather and altitude scenarios

Four environmental cases are analysed. Fair weather uses m = 0.85 and heavy rain uses m = 0.60, and each is evaluated at sea level (δ = 1.000) and at 2000 m (δ = 0.788). At altitude the air is thinner and the onset gradient falls accordingly. The weather-weighted corona loss is the time-weighted average Pcor = (1 − xf) Pfair + xf Prain, with a foul-weather fraction xf of 10% in the base case and 5–30% in

the sensitivity analysis. The 10% value is an assumed adverse-weather fraction, not a measured annual probability. The two-state weather model also does not resolve rain intensity, fog, humidity, pollution, dust accumulation, surface roughness, conductor ageing or local field enhancement at fittings and spacers [4], [5]. It is therefore suitable for comparative screening only; annual loss estimates require site-specific meteorological and condition records together with a load-duration profile.

Computational procedure

For each configuration the calculation has five steps. (1) Compute the equivalent phase capacitance and the representative peak surface gradient from Eq. (3). (2) Compute the onset gradient and critical voltage for each weather case from Eqs. (1), (2) and (4). (3) Evaluate the corona loss from Eq. (5) whenever Vph > V0. (4) Compute Rac from Eqs. (7)–(8) at the fixed operating temperature, using the effective-conductor approximation described in Section 2.2. (5) Combine the results through Eq. (9) to obtain the configuration-level efficiency. All calculations were implemented in Python (NumPy/SciPy), and the Bessel-function solution for a homogeneous solid conductor served as an independent consistency check on the IEC expression; it does not validate the omitted strand-level and steel-core effects in ACSR. No phase-specific electrostatic solution, shield-wire model, hardware field-enhancement factor or time-series weather/load simulation was applied.

RESULTS AND DISCUSSION

Skin effect

Table 1 shows that the effective-conductor calculation raises the conductor resistance by only 0.30% for Panther and 1.20% for Zebra at 75 °C and 50 Hz. The proximity contribution in the twin bundle is 0.03%, which is negligible at 0.40 m spacing within this model. As Fig. 1 shows, the skin-effect factor climbs as the dc resistance falls, that is, as the conductor gets larger. It is also roughly 40–45% higher at 60 Hz than at 50 Hz for the same conductor, because it scales approximately with the square of frequency. These results establish that skin effect is included in the loss accounting, but they also show that it is not a first-order efficiency driver for the present 50 Hz line: its resistance increase is at most 1.20%, and its effect must be compared with the much larger baseline Joule loss. The trend should not be extrapolated to detailed ACSR behaviour without a strand- and core-resolved model.

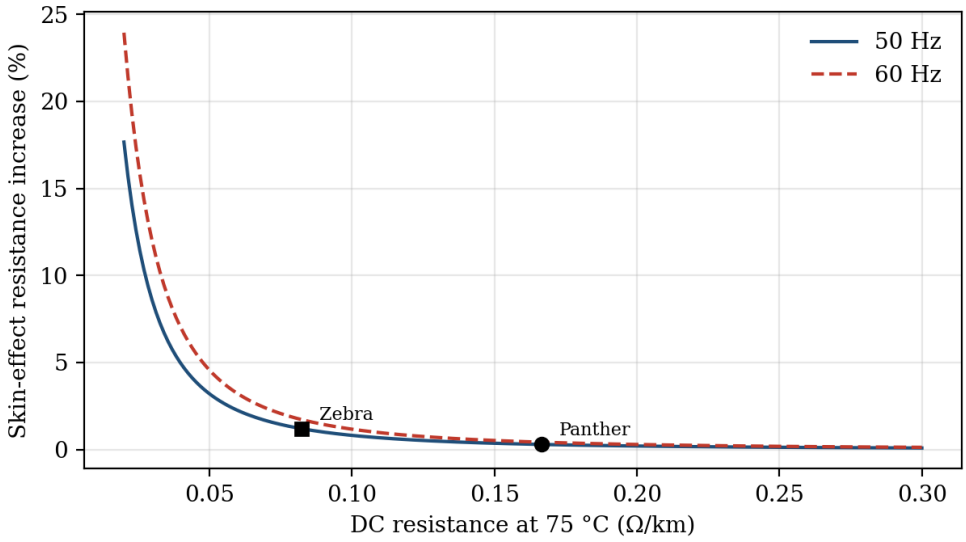


Figure 1. Skin-effect resistance increase versus dc resistance at 75 °C for 50 Hz and 60 Hz systems. The markers indicate the conductors studied.

An independent consistency check supports the effective-conductor values, but its scope is limited. The exact Bessel-function solution for a solid aluminium rod with the same cross-sectional area as Zebra (428.9 mm², radius 11.68 mm) gives a resistance ratio of 1.0126 at 75 °C, against 1.0120 from the IEC

expression for Zebra. The two agree to within 0.1% for the corresponding homogeneous-conductor problem. This agreement verifies the implementation of the screening approximation; it does not establish that an ACSR conductor has the same current distribution, because the steel core, radial aluminium layers and helical strand lay remain unresolved [7,9,12].

Corona onset and corona loss

Figure 2 compares the representative peak surface gradient with the onset gradients. At 220 kV and sea level, single Zebra operates at 19.77 kV/cm. That is well below the fair-weather onset of 25.5 kV/cm but above the heavy-rain onset of 18.0 kV/cm. Panther, with its smaller radius, operates at 25.69 kV/cm, essentially at the fair-weather onset, so even a slight rise in voltage or altitude should produce corona in the equivalent-geometry calculation. The twin Zebra bundle lowers the representative gradient to 14.36 kV/cm, which is below both thresholds at nominal voltage. Because the calculation assigns one Emax to all phases and excludes shield wires, fittings, spacers, contamination and ageing, these margins are screening margins rather than phase-resolved acceptance limits; local hardware can produce a higher field than the smooth-conductor value [4,5].

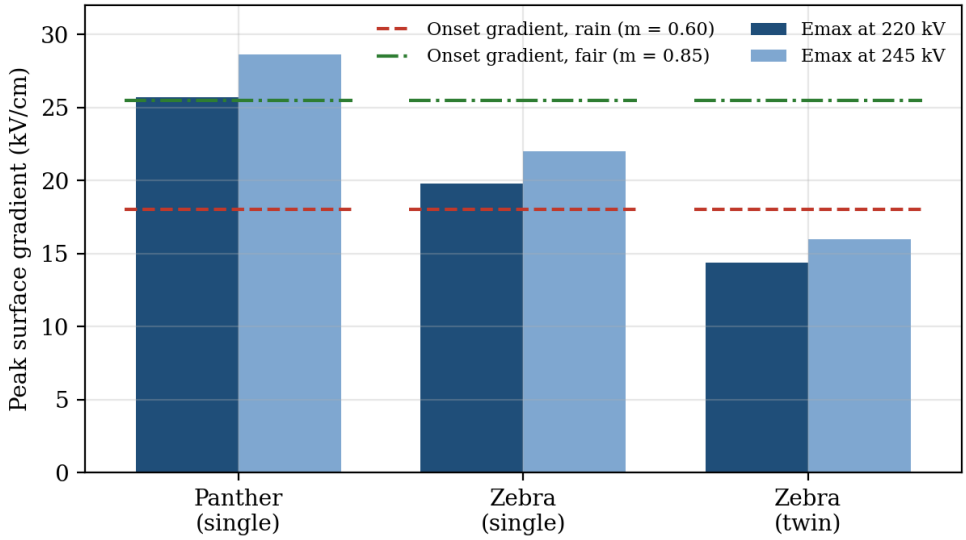


Figure 2. Peak conductor surface gradient at 220 kV and 245 kV compared with the onset gradient in fair weather and in heavy rain (sea level).

Table 2. Corona onset and three-phase corona loss (kW/km) for the studied configurations at sea level

Configuration	V_0 fair (kV)	V_0 rain (kV)	P_c fair, 220 kV	P_c rain, 220 kV	P_c rain, 245 kV
Single ACSR Panther	126.0	89.0	0.02	28.11	53.49
Single ACSR Zebra	163.8	115.6	0.00	2.95	15.13
Twin ACSR Zebra (0.40 m)	225.5	159.2	0.00	0.00	0.00

V_0: critical phase-to-neutral voltage (rms). Nominal phase voltage at 220 kV is 127.0 kV and at 245 kV is 141.4 kV. Losses are three-phase totals per kilometre.

The loss results in Table 2 follow the representative-gradient ranking. In heavy rain at 220 kV, the corona loss is 28.1 kW/km for Panther, 2.95 kW/km for single Zebra and zero for twin Zebra. Raising the voltage to 245 kV increases the single Zebra loss roughly fivefold, to 15.1 kW/km, and at 2000 m it produces fair-weather corona for single Zebra (4.4 kW/km at 245 kV). Figure 3 shows that once the critical voltage is exceeded the loss grows steeply, approximately quadratically, which makes voltage regulation an indirect but effective means of corona control. These numerical values describe the smooth, phase-averaged analytical model; contamination, hardware protrusions and phase-specific field concentration can shift the onset and change the measured loss, so the values should not be treated as calibrated field predictions [4,5].

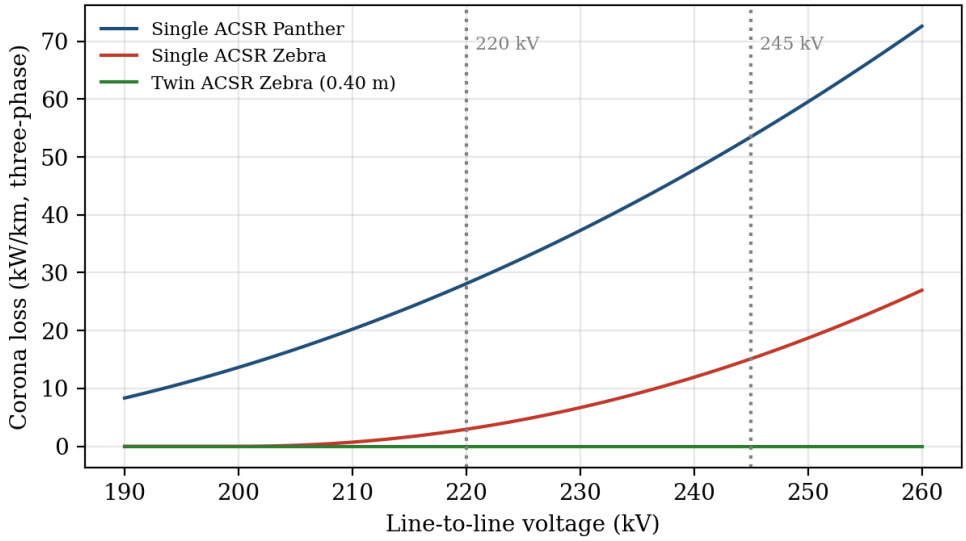


Figure 3. Three-phase corona loss versus line-to-line voltage in heavy rain at sea level (m = 0.60).

Combined effect on transmission efficiency

Table 3 breaks down the efficiency at 150 MW (current 414.4 A) for the sea-level case with 10% assumed foul-weather time. Joule heating in the conductors dominates, ranging from 2.12 MW for twin Zebra to 8.58 MW for Panther. The effective-conductor skin correction adds only 0.025–0.051 MW, which lowers efficiency by 0.015–0.032 percentage points. The weather-weighted corona loss is 0.283 MW for Panther, 0.029 MW for single Zebra and zero for twin Zebra. This comparison resolves the conceptual issue in the title and objectives: for the present 50 Hz, 220 kV cases, skin effect is a completeness check on ac resistance, not a practically dominant loss mechanism. Corona exceeds the skin-effect penalty for Panther, while both effects remain smaller than the baseline conductor loss. The conclusion is conditional on the stated geometry, temperature and weather weighting.

Table 3. Loss decomposition and efficiency at 150 MW, 100 km, power factor 0.95, sea level, 10% foul-weather time

Configuration	I (A)	$P_{Cu,dc}$ (MW)	Skin ΔP (MW)	$P_{cor,avg}$ (MW)	η_{dc} (%)	η_{ac} (%)	η total / rain (%)
Single ACSR Panther	414.4	8.577	0.025	0.283	94.59	94.58	94.41 / 92.93
Single ACSR Zebra	414.4	4.241	0.051	0.029	97.25	97.22	97.20 / 97.03
Twin ACSR Zebra (0.40 m)	414.4	2.121	0.026	0.000	98.61	98.59	98.59 / 98.59

η_{dc}: efficiency with dc resistance only; η_{ac}: with skin and proximity effects; "total" includes weather-weighted corona; "rain" is the efficiency during heavy rain only

Expressed as annualized energy under the artificial assumption of a constant 150 MW load, skin effect amounts to roughly 222 MWh for Panther, 446 MWh for single Zebra and 228 MWh for twin Zebra. Weather-weighted corona amounts to about 2,477 MWh, 258 MWh and 0 MWh respectively. For single Zebra the two incremental mechanisms are of comparable order in this assumed weighting, but both are far smaller than the baseline conductor loss of about 37,154 MWh. These are scenario conversions rather than annual forecasts because the model uses a fixed load, fixed 75 °C conductor temperature and assumed weather fractions. During a heavy-rain event, however, the instantaneous efficiency of the single-conductor lines drops visibly, to 92.93% for Panther and 97.03% for Zebra, while twin Zebra is unaffected within the idealized model.

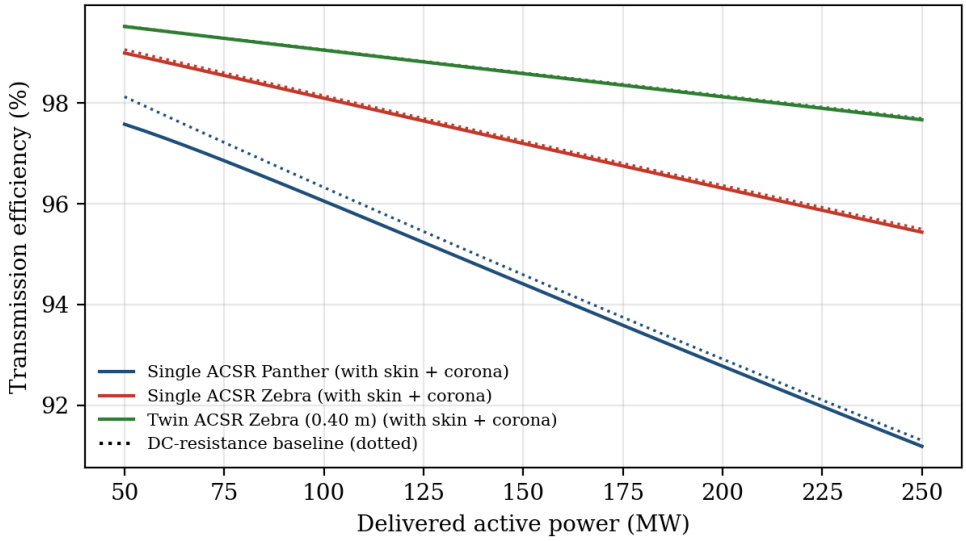


Figure 4. Transmission efficiency versus delivered power for the three configurations (sea level, 10% foul-weather time). Dotted lines show the dc-resistance baseline without skin effect and corona.

Figure 4 shows that the efficiency gap between the configurations is governed mainly by the number and size of the conductors. The gap widens with load, because conductor loss scales with the square of the current. Corona is visible only for Panther at light load, where it is a constant loss on top of a small conductor loss; the gap between the solid and dotted Panther curves is therefore largest at 50 MW and narrows as Joule loss grows. Skin-effect differences cannot be resolved at the scale of the figure, reinforcing that the skin correction is not the primary design discriminator at 50 Hz. In an installed line, local hardware and surface condition could add corona losses that are absent from these smooth-conductor curves.

Altitude and foul-weather sensitivity

At 2000 m the air density factor falls to 0.788, and the onset gradients drop by about 21%. Table 4 shows that corona then becomes significant even for single Zebra in heavy rain (37.1 kW/km) and for Panther in all conditions (18.9 kW/km in fair weather). The weather-weighted corona loss for Panther reaches 2.50 MW, lowering the efficiency to 93.11% from 94.58% without corona. Twin Zebra remains largely unaffected (0.001 MW). Varying the assumed foul-weather fraction from 5% to 30% lowers the efficiency of single Zebra at altitude from 97.10% to 96.52%, and that of Panther from 93.29% to 92.41%. These values demonstrate sensitivity to altitude and the chosen scenario weight; they are not a substitute for a site-specific annual assessment that includes load duration, conductor temperature, pollution, surface ageing and local hardware fields. Site climate is nevertheless a first-order design input where corona is concerned.

Table 4. Efficiency at 150 MW, 100 km, 2000 m altitude (δ = 0.788), 10% foul-weather time

Configuration	P_c fair (kW/km)	P_c rain (kW/km)	$P_{cor,avg}$ (MW)	η total (%)	η rain (%)
Single ACSR Panther	18.88	79.77	2.497	93.11	90.05
Single ACSR Zebra	0.00	37.06	0.371	96.99	94.94
Twin ACSR Zebra (0.40 m)	0.00	0.14	0.001	98.59	98.58

The altitude results for Panther and single Zebra should be read as screening values, not as validated upper bounds for an installed line. Peek-type formulas can depart from measured loss at large ratios of V/V0, and for Panther in heavy rain at altitude the ratio approaches 1.8. In addition, the present calculation omits phase asymmetry, shield-wire and ground-plane coupling, conductor contamination and ageing, and local field enhancement at fittings and bundle spacers. The qualitative conclusion is

robust within the model: small single conductors are unsuitable at 220 kV in high-altitude or wet climates. The numerical loss values should, however, be validated with conductor-specific electromagnetic calculations, laboratory or field measurements, and a time-series operating model before they are used in an economic evaluation.

DISCUSSION

Four points stand out. First, the efficiency of a 220 kV line is overwhelmingly set by baseline conductor resistance, that is, by the cross-section and number of subconductors. Reducing corona or skin effect cannot compensate for an undersized conductor. Second, the skin-effect calculation is useful for completeness and for comparing conductor sizes, but its practical impact is negligible in the present 50 Hz cases: resistance increases by no more than 1.2% and efficiency decreases by only 0.015–0.032 percentage points. The title and objectives should therefore not be read as implying equal practical importance for the two mechanisms. Third, corona is a threshold phenomenon. Designs with sufficient gradient margin lose almost nothing in the idealized model, whereas designs close to the threshold can lose substantially more in foul weather. Fourth, phase asymmetry, shield wires, fittings, spacers, pollution, ageing and time-varying operation can move the actual margin away from the present screening result. Bundling or a larger conductor diameter is therefore usually specified at 220 kV not to eliminate skin effect, but to create robust corona margin while satisfying thermal and mechanical constraints.

MITIGATION AND DESIGN RECOMMENDATIONS

1. Control the surface gradient. Use larger-diameter or bundled conductors. The twin Zebra arrangement cut the representative gradient from 19.8 to 14.4 kV/cm and removed corona in all sea-level scenarios in the analytical model. For final design, calculate the field separately for each phase and include the ground plane, shield wires, fittings and bundle spacers; expanded or hollow conductors can achieve a similar reduction with a smaller weight penalty.
2. Allow for altitude and climate. Apply the air-density correction at the design stage, and size conductors against the heavy-rain onset gradient rather than the fair-weather value, particularly above about 1000 m or in high-rainfall regions. Replace the assumed 10% adverse-weather fraction with site observations or a validated climatic distribution when annual energy loss is required.

3. Limit voltage excursions. Corona loss rises sharply after onset, so reactive-power and tap-changer control that keeps the voltage close to nominal reduces losses. The control margin should be checked against the highest-field phase rather than the phase-averaged value used here.

4. Treat skin effect proportionately when choosing conductors. At 50 Hz for the present conductor sizes it is a secondary correction, not a primary efficiency driver; nevertheless, frequency, operating temperature, strand geometry and the magnetic steel core should be included through a conductor-specific ac-resistance model when high-accuracy loss estimates are needed [6,7].

5. Maintain the surface condition and hardware geometry. Inspect for dust, industrial pollution, corrosion, surface damage and ageing; use corona rings and smooth fittings; and control the geometry of suspension fittings, clamps and bundle spacers to limit local field enhancement. These effects should be represented by local-field factors or verified experimentally rather than inferred from the smooth-conductor Emax alone [4, 5,13].

Limitations and Future Work

This study is an analytical screening assessment and rests on empirical formulas whose accuracy is limited, especially for bundled conductors, contaminated surfaces and high ratios of V/V0. The ground plane and overhead shield wires are omitted, and the same representative gradient is applied to all phases; consequently, the higher or differently distributed field that can occur on the centre phase of a

horizontal arrangement is not resolved. Local field intensification at suspension fittings, clamps, corona rings and bundle spacers is also excluded. The corona model does not represent dust accumulation, industrial pollution, surface roughness, conductor ageing or degradation, and the two-state weather model with a fixed 10% foul-weather fraction is not an annual climatic model. The line is evaluated at a fixed 150 MW base case and a fixed 75 °C conductor temperature rather than a time-varying load-temperature profile. Finally, skin effect in ACSR is represented by an effective solid-conductor approximation; the magnetic steel core, radial current redistribution among aluminium layers and helical strand lay are not explicitly modelled [6,7,11]. These limitations mean that the numerical efficiencies and corona losses should not be used directly for procurement or economic decisions. Future work should solve the phase- and shield-wire electrostatic geometry, use a conductor-specific stranded-ACSR impedance model, include local hardware field factors and surface-condition states, validate the results against laboratory or field measurements, and apply synchronized time-series weather, pollution, loading and conductor-temperature data to calculate annual energy loss.

CONCLUSIONS

This paper evaluated corona discharge and the skin-effect contribution to the efficiency of a 220 kV, 100 km transmission line using a unified analytical screening model. The main findings are as follows. (i) At 50 Hz and 75 °C, the effective-conductor calculation raises resistance by 0.3% for Panther and 1.2% for Zebra, but lowers efficiency by only 0.015–0.032 percentage points at 150 MW; skin effect is therefore a secondary correction rather than a dominant practical loss. (ii) Corona is negligible in fair weather at sea level for the Zebra-based designs, but in heavy rain it reaches 28.1 kW/km for Panther and 2.95 kW/km for single Zebra. (iii) Altitude and voltage excursions raise the corona risk substantially; at 2000 m a single small conductor can lose about 1.5 percentage points of efficiency on the stated weather-weighted scenario. (iv) The twin Zebra bundle stays essentially corona-free at nominal voltage and achieves the highest efficiency, 98.59% at 150 MW, within the equivalent-geometry model. These conclusions are conditional because the analysis does not resolve centre-phase asymmetry, shield wires, local hardware enhancement, contamination and ageing, stranded-ACSR current redistribution, or time-varying weather, load and temperature. For practical 220 kV design, phase-resolved field analysis and site-specific environmental data should therefore be used; within the present screening scope, sizing and bundling conductors to keep the surface gradient below the heavy-rain onset value is more effective than attempting to reduce the already small skin-effect correction.

Declarations

Conflict of interest: The authors declare no conflict of interest.

Funding: “None”.

Data availability: All input data are given in Table 1 and Section 3; the calculation procedure is fully described by Eqs. (1)–(9).

REFERENCES

1. J. J. Grainger and W. D. Stevenson, *Power System Analysis*. New York, NY, USA: McGraw-Hill, 1994.
2. P. Kundur, *Power System Stability and Control*. New York, NY, USA: McGraw-Hill, 1994.
3. F. W. Peek, *Dielectric Phenomena in High Voltage Engineering*, 3rd ed. New York, NY, USA: McGraw-Hill, 1929.
4. Electric Power Research Institute, *Transmission Line Reference Book: 345 kV and Above*, 2nd ed. Palo Alto, CA, USA: EPRI, 1982.
5. P. S. Maruvada, *Corona Performance of High-Voltage Transmission Lines*. Baldock, U.K.: Research Studies Press, 2000.

6. IEC 60287-1-1, *Electric Cables – Calculation of the Current Rating – Part 1-1: Current Rating Equations (100% Load Factor) and Calculation of Losses – General*, International Electrotechnical Commission, Geneva, Switzerland.
7. IEC 61597, *Overhead Electrical Conductors – Calculation Methods for Stranded Bare Conductors*, International Electrotechnical Commission, Geneva, Switzerland, 1995.
8. IEEE Std 738-2012, *IEEE Standard for Calculating the Current-Temperature Relationship of Bare Overhead Conductors*, IEEE, New York, NY, USA, 2012.
9. J. A. Stratton, *Electromagnetic Theory*. New York, NY, USA: McGraw-Hill, 1941.
10. Najeeb Ahmed , O., & Amer Mohammed, A. (2026). Intelligent Deep Learning-based Systems to Detect Early Cyber Attacks in IoT Networks. Libyan Journal of Applied and Contemporary Sciences, 1(1), 38–52. https://doi.org/10.64943/ljacs.2026.010105
11. J. R. Carson, "Wave propagation in overhead wires with ground return," *Bell Syst. Tech. J.*, vol. 5, no. 4, pp. 539–554, 1926.
12. CIGRÉ Working Group 22.12, *Thermal Behaviour of Overhead Conductors*, CIGRÉ Technical Brochure 207, 2002.
13. A. R. Bergen and V. Vittal, *Power Systems Analysis*, 2nd ed. Upper Saddle River, NJ, USA: Prentice Hall, 2000.
14. Akram, M., Khudhair Hasan, M., Abdulghafoor, H. A., Saidan, F., Ahmet Ozdemir, F., Sołowski, G., & Bin Ali, J. (2026). Health, Science, and Sustainability: A Multidisciplinary Review of Disease Dynamics, Therapeutic Advances, and Environmental Challenges. Libyan Journal of Applied and Contemporary Sciences, 1(1), 1–9. https://doi.org/10.64943/ljacs.2026.010101

تقييم تحليلي لمساهمة التفريغ الهالي (Corona Discharge) والتأثير السطحي (Skin Effect) في كفاءة خطوط النقل الهوائية ذات الجهد 220 كيلوفولت

ملخص

يُعد التفريغ الهالي أحد آليات الفقد الرئيسية في خطوط النقل الهوائية ذات الجهد العالي، بينما يُتوقع أن يكون تأثير الظاهرة السطحية (Skin Effect)عند تردد 50 هرتز ثانوياً بالنسبة لأحجام الموصلات المدروسة هنا. تقدم هذه الورقة تقديراً كمياً لكلا التأثيرين لخط نقل بجهد 220 كيلوفولت، وتردد 50 هرتز، وطول 100 كيلومتر، وذلك باستخدام نموذج تحليلي تقييمي. تجري المقارنة بين ثلاثة تكوينات للأطوار: موصل مفرد من نوع "Panther" من طراز(ACSR ، وموصل مفرد من نوع "Zebra" من طراز(ACSR ، وتكوين مزدوج (Twin-bundle) من نوع "Zebra". تم حساب تدرجات الجهد السطحي (Surface Gradients) بناءً على هندسة أفقية مكافئة، ومقارنتها بتدرجات الجهد اللازمة لبدء التفريغ الهالي في ظروف الطقس الصحو والأمطار الغزيرة، وذلك عند مستوى سطح البحر وعلى ارتفاع 2000 متر. قُدِّرت فواقد التفريغ الهالي باستخدام معادلة "بيك(Peek's formula) "، بينما حُسبت مقاومة التيار المتردد وفقاً لمعايير اللجنة الكهرتقنية الدولية (IEC 60287) المتعلقة بالتأثير السطحي وتأثير القرب(Proximity Effect) ، مع التحقق من النتائج باستخدام حل يعتمد على دوال "بيسل (Bessel functions) "للموصلات المصمتة. عند حمل قدره 150 ميجاوات ومعامل قدرة 0.95، يؤدي التأثير السطحي إلى زيادة مقاومة الموصل بنسبة 0.30% لنوع "Panther" وبنسبة 1.20% لنوع"Zebra" ، مما يقلل الكفاءة بمقدار يتراوح بين 0.015% و0.032% فقط. وفي ظروف الطقس الصحو عند مستوى سطح البحر، تكون فواقد التفريغ الهالي مهملة لكلا تصميمي ."Zebra" أما في حالات الأمطار الغزيرة، فتصل هذه الفواقد إلى 28.1 كيلوواط/كم لموصل "Panther" و2.95 كيلوواط/كم لموصل "Zebra" المفرد، وتزداد بشكل حاد عند الارتفاعات العالية أو عند ارتفاع الجهد ليصل إلى 245 كيلوفولت. أما التكوين المزدوج من نوع "Zebra" فيظل خالياً من التفريغ الهالي عند الجهد الاسمي في جميع السيناريوهات عند مستوى سطح البحر، محققاً أعلى كفاءة بنسبة 98.59%. ونظراً لأن النموذج يتجاهل -عن قصد- عوامل مثل عدم تماثل المجال الكهربائي الخاص بكل طور، والأسلاك الحامية(Shield wires) ، والتحسينات الهندسية الموضعية، وتلوث سطح الموصلات، بالإضافة إلى التغيرات الزمنية في الطقس والأحمال ودرجات الحرارة؛ فإن النتائج الرقمية المستخلصة يجب أن تُفهم كقيم تقديرية أولية. وفي هذا السياق، يتضح أن اختيار نوع الموصل، واستخدام التكوينات المزدوجة، ومراعاة تأثير الارتفاع على الأداء، هي العوامل التي تحدد حجم الفواقد الناتجة عن التفريغ الهالي، بينما أُدرج التأثير السطحي بشكل أساسي لتوضيح مساهمته العملية المحدودة.

الكلمات المفتاحية: خط نقل 220 كيلوفولت؛ فقد الهالة؛ تأثير الجلد؛ كفاءة النقل؛ موصلاتACSR ؛ موصلات مجمعة؛ صيغة بيك